dropping below this threshold, we setup and evaluate the following integral:

$$
\begin{aligned}
\Pr[0 \leq R < 0.3162\sqrt{P_{\mathrm{dif}}}] &= \int_{0}^{0.3162\sqrt{P_{\mathrm{dif}}}} \frac{2\rho}{P_{\mathrm{dif}}} \exp\left(\frac{-\rho^2}{P_{\mathrm{dif}}}\right) d\rho \\
&= -\exp\left(\frac{-\rho^2}{P_{\mathrm{dif}}}\right)\Bigg|_{0}^{\rho=0.3162\sqrt{P_{\mathrm{dif}}}} \\
&= 0.0952
\end{aligned}
$$

If we assume that fades are slow with respect to data packet length, we can estimate that 9.5% of the packets will be dropped.

5.3.5 The Rician PDF

The Rician PDF describes the fading of nonspecular power in the presence of a dominant, nonfluctuating multipath component [Reu74], [Ric48]. The analytical expression for the Rician distribution results from the integration of Equation (5.2.13) under the condition $N = 1$ and nonzero P_{dif}. After applying a well-understood definite integral relationship [Gra94, p. 739], the resulting PDF is

$$
f_R(\rho) = \frac{2\rho}{P_{\mathrm{dif}}} \exp\left(\frac{-\rho^2 - V_1^2}{P_{\mathrm{dif}}}\right) \mathrm{I}_0\left(\frac{2\rho V_1}{P_{\mathrm{dif}}}\right), \quad \rho \geq 0 \tag{5.3.7}
$$

where $\mathrm{I}_0(\cdot)$ is a zero-order modified Bessel function. An IQ sketch of the Rician PDF is shown in Figure 5.5.

Figure 5.6 shows several different kinds of Rician PDFs and CDFs. The plots are labeled using a Rician K factor, which is the ratio of the power of the dominant multipath component to the power of the remaining nonspecular multipath:

$$
K = \frac{\text{Specular Power}}{\text{Nonspecular Power}} = \frac{V_1^2}{P_{\mathrm{dif}}} \tag{5.3.8}
$$

In the literature, the parameter K is often given as a dB value, which is $10\log_{10}$ of the quantity in Equation (5.3.8). Notice from Figure 5.6 that $K = -\infty$ dB corresponds to the Rayleigh PDF and the complete disappearance of the specular power.

> *Note: A Useful Approximation*
>
> As the Rician K-factor becomes large ($K \gg 1$), it is possible to approximate the Rician distribution with a Gaussian PDF of the following form:
>
> $$f_R(\rho) = \frac{1}{\sqrt{\pi P_{\mathrm{dif}}}} \exp\left(-\frac{(\rho - V_1)^2}{P_{\mathrm{dif}}}\right)$$

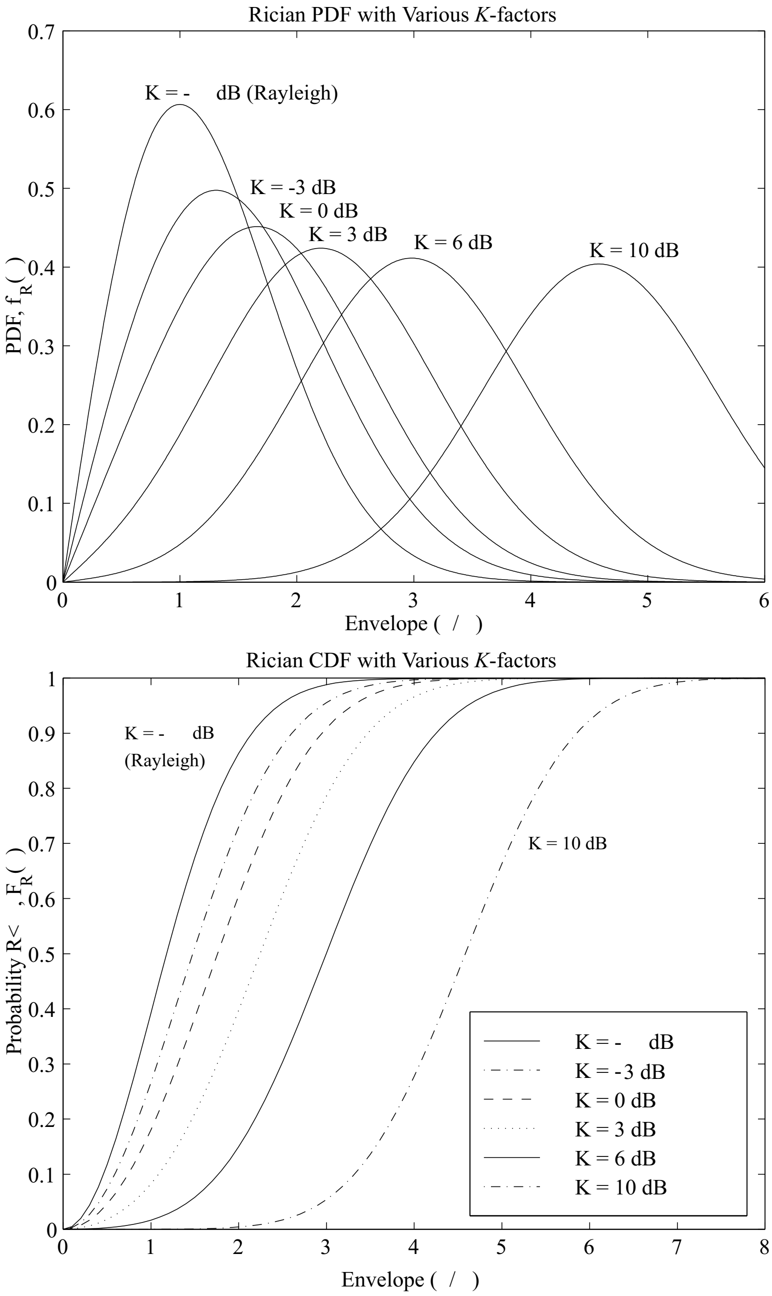

Figure 5.6 Rician PDF and CDF as the dominant multipath component increases ($\sigma = \sqrt{P_{\text{dif}}/2}$) [Dur02].

> *Note: Rice or Nakagami*
>
> The Rician distribution is also called the *Rice-Nakagami* distribution in the literature to recognize the result that was independently formulated by outstanding Japanese researcher M. Nakagami. The term *Rician* is used in this work not to diminish Nakagami's contribution, but to avoid confusion with another popular PDF in radio channel modeling that bears his name: the *Nakagami-m* distribution [Nak60]. This distribution was originally formulated for characterizing temporal fading measurements from upper-atmosphere propagation but has been applied liberally to the small-scale fading of terrestrial wireless systems as well [Cou98a], [Yac00].

5.4 Two-Wave with Diffuse Power PDF

If Equation (5.2.13) is evaluated with $N = 2$ and nonzero P_{dif}, then the two-wave with diffuse power (TWDP) PDF results [Esp73], [Dur02]. Such a distribution, while difficult to model analytically, provides the greatest wealth of fading behavior for an I-SLAC model.

5.4.1 Approximate Representation

We will use parameters similar to the physical Rician K-parameter of Equation (5.3.8) and the two-wave Δ-parameter of Equation (5.3.3) to classify the shape of the TWDP PDF:

$$K = \frac{V_1^2 + V_2^2}{P_{\text{dif}}} \qquad \Delta = \frac{2V_1V_2}{V_1^2 + V_2^2} \tag{5.4.1}$$

There is no exact closed-form equation for TWDP fading, but this section presents a family of closed-form PDFs that closely approximate the behavior of the exact TWDP PDF.

An IQ sketch of TWDP fading is shown in Figure 5.7. One common approximation to the TWDP PDF is presented in [Dur02]:

$$f_R(\rho) = \frac{2\rho}{P_{\text{dif}}} \exp\left(\frac{-\rho^2}{P_{\text{dif}}} - K\right) \sum_{i=1}^{M} a_i \mathrm{D}\left(\frac{\rho}{\sqrt{P_{\text{dif}}/2}}; K, \Delta\cos\frac{\pi(i{-}1)}{2M{-}1}\right) \tag{5.4.2}$$

where

$$\mathrm{D}\left(x; K, \alpha\right) = \frac{1}{2}\exp(\alpha K)\mathrm{I}_0\left(x\sqrt{2K(1-\alpha)}\right) + \frac{1}{2}\exp(-\alpha K)\mathrm{I}_0\left(x\sqrt{2K(1+\alpha)}\right).$$

The value M in the summation is the *order* of the approximate TWDP PDF. By increasing the order in Equation (5.4.2), the approximate PDF becomes a more accurate representation of the true TWDP PDF. However, using the first few orders ($M = 1$ through 5) yields accurate representations *over the most useful range of K and Δ parameters.* Table 5.2 records the exact $\{a_i\}$ coefficients for the first five orders of Equation (5.4.2).

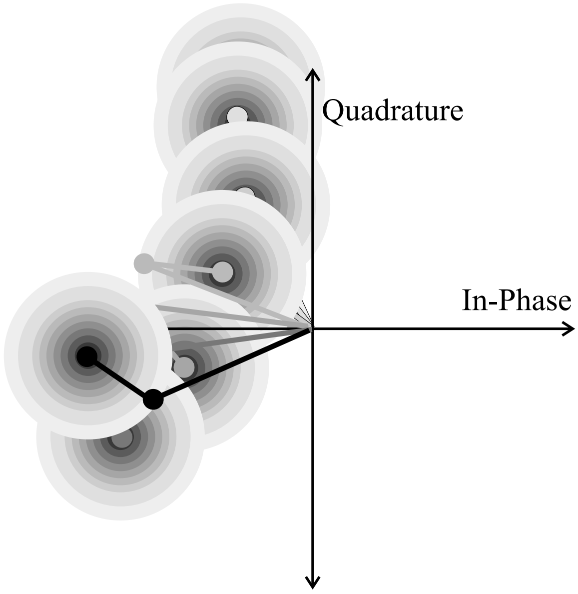

Figure 5.7 A diffuse, Rayleigh component added to two randomly phased specular waves to produce a TWDP distribution.

Table 5.2 Exact Coefficients for the First Five Orders of the Approximate TWDP Fading PDF

Order	a_1	a_2	a_3	a_4	a_5
1	1				
2	$\frac{1}{4}$	$\frac{3}{4}$			
3	$\frac{19}{144}$	$\frac{25}{48}$	$\frac{25}{72}$		
4	$\frac{751}{8640}$	$\frac{3577}{8640}$	$\frac{49}{320}$	$\frac{2989}{8640}$	
5	$\frac{2857}{44800}$	$\frac{15741}{44800}$	$\frac{27}{1120}$	$\frac{1209}{2800}$	$\frac{2889}{22400}$

The product of the parameters K and Δ determines which order of Equation (5.4.2) should be used when representing TWDP fading. As the product of these two parameters increases, a higher order approximation is needed to model the TWDP PDF accurately. As a general rule of thumb, the minimum order is

$$\text{Order } (M) = \left\lceil \frac{1}{2} K \Delta \right\rceil \tag{5.4.3}$$

where $\lceil \cdot \rceil$ is the ceiling function (round up). Equation (5.4.3) is based on a graphical comparison between the approximate analytical functions and the true, numerical solution of the TWDP PDF. The approximate PDF will deviate from the exact TWDP PDF only if the specular power is much larger than the nonspecular power (large K value) *and* if the amplitudes of the specular voltage components are relatively equal in magnitude (Δ approaches 1).

Example 5.3: Order-2 Approximate TWDP PDF

Problem: Using Table 5.2 and Equation (5.4.2), calculate the order-2 approximate TWDP PDF.

Solution: Plugging the coefficients a_1 and a_2 into Equation (5.4.2) produces

$$f_R(\rho) = \frac{2\rho}{P_{\text{dif}}} \exp\left(\frac{-\rho^2}{P_{\text{dif}}} - K\right)\left[\frac{1}{4}\mathrm{D}\left(\frac{\rho}{\sqrt{P_{\text{dif}}/2}}; K, \Delta\right) + \frac{3}{4}\mathrm{D}\left(\frac{\rho}{\sqrt{P_{\text{dif}}/2}}; K, \frac{\Delta}{2}\right)\right]$$

which, in this form, is not much more complicated than a Rician PDF.

Despite being an approximate result, the family of PDFs in Equation (5.4.2) have a number of extraordinary characteristics that are independent of order, M, and parameters, K and Δ:

- *They are mathematically exact PDFs.* They integrate to 1 over the range $0 \leq \rho < \infty$.
- *They are accurate over their upper and lower tails.* These regions are important for modeling noise-limited or interference-limited mobile communication systems [Cou98b].
- *They all exactly preserve the second moment of the true PDF.* The second moment is the most important moment to preserve, since it physically represents the average local area power [Rap02a].
- *They can be entirely described with three physically intuitive parameters.* The physical parameters P_{dif}, K, and Δ - as defined in this book - have straightforward physical definitions.
- *They exhibit the proper limiting behavior.* All of the PDFs contain, as a special case of $\Delta = 0$, the exact Rician PDF and, as a special case of $K = 0$, the exact Rayleigh PDF.

Accurate analytical representation of these PDFs reveals interesting behavior in fading channels that goes unnoticed using Rician PDFs, which are capable of modeling the envelope fading of diffuse power in the presence of only *one* specular component.

It should be noted that there are many interesting ways to approximate the TWDP PDF and other nonanalytic forms of Equation (5.2.13) (see the work by Esposita and Wilson in [Esp73] and Abdi et al. in [Abd00]).

5.4.2 Graphical Analysis

Figures 5.8 through 5.11 plot a series of PDFs and CDFs for TWDP fading. As shown by Figure 5.8, there is little difference between the Rician PDF and the TWDP PDF when K is less than 3 dB. The difference gradually becomes more pronounced as K increases, particularly when the specular power is divided equally between the two discrete components ($\Delta = 1$). The $K = 10$ dB graph of Figure 5.11 illustrates these distortions most dramatically. In fact, as the product of parameters K and Δ becomes large, the graph of the PDF becomes bimodal, exhibiting two maxima.

5.4.3 Rayleigh and Rician Approximations

For the limiting parameter cases of Table 5.3, the exact TWDP PDF contains the Rayleigh, Rician, one-wave, and two-wave PDFs. This demonstrates the generality of the exact and approximate TWDP PDFs. It also shows the utility of the three-wave PDF, since it is the only analytical expression in Table 5.1 that is not a general case of the TWDP PDF.

Table 5.3 The TWDP PDF Contains the Rayleigh, Rician, One-Wave, and Two-Wave PDFs as Special Cases

Parameter Value		Type of Fading
$K = 0$	–	Rayleigh
$K > 0$	$\Delta = 0$	Rician
$K \to \infty$	$\Delta = 0$	One-Wave
$K \to \infty$	$\Delta > 0$	Two-Wave

Since the Rician and Rayleigh PDFs are special cases of the TWDP PDF, it is useful to know the range of parameters over which TWDP fading may be approximated by these simpler distributions. An inspection of the graphs of Figure 5.8 through Figure 5.11 reveals the range of K and Δ over which a Rician PDF approximates a TWDP PDF. In general, the TWDP PDF resembles a Rician PDF in shape for $K\Delta < 2$. Under this condition, the smallest of the two specular components may be grouped with the nonspecular power so that only one large specular component remains. After computing a Rician K-factor for this new grouping, the resulting Rician PDF will approximately describe the envelope of the TWDP fading.

TWDP fading may be further approximated by a Rayleigh PDF if, in addition to the above-mentioned criterion, the power of the largest specular component is less than the power of the smaller specular component *plus* the average nonspecular power:

$$\begin{aligned} \max(V_1^2, V_2^2) \;&<\; \min(V_1^2, V_2^2) + P_{\text{dif}} \\ \frac{1}{2} + \frac{1}{2}\sqrt{1-\Delta^2} \;&<\; \frac{1}{2} - \frac{1}{2}\sqrt{1-\Delta^2} + \frac{1}{K+1} \end{aligned} \tag{5.4.4}$$

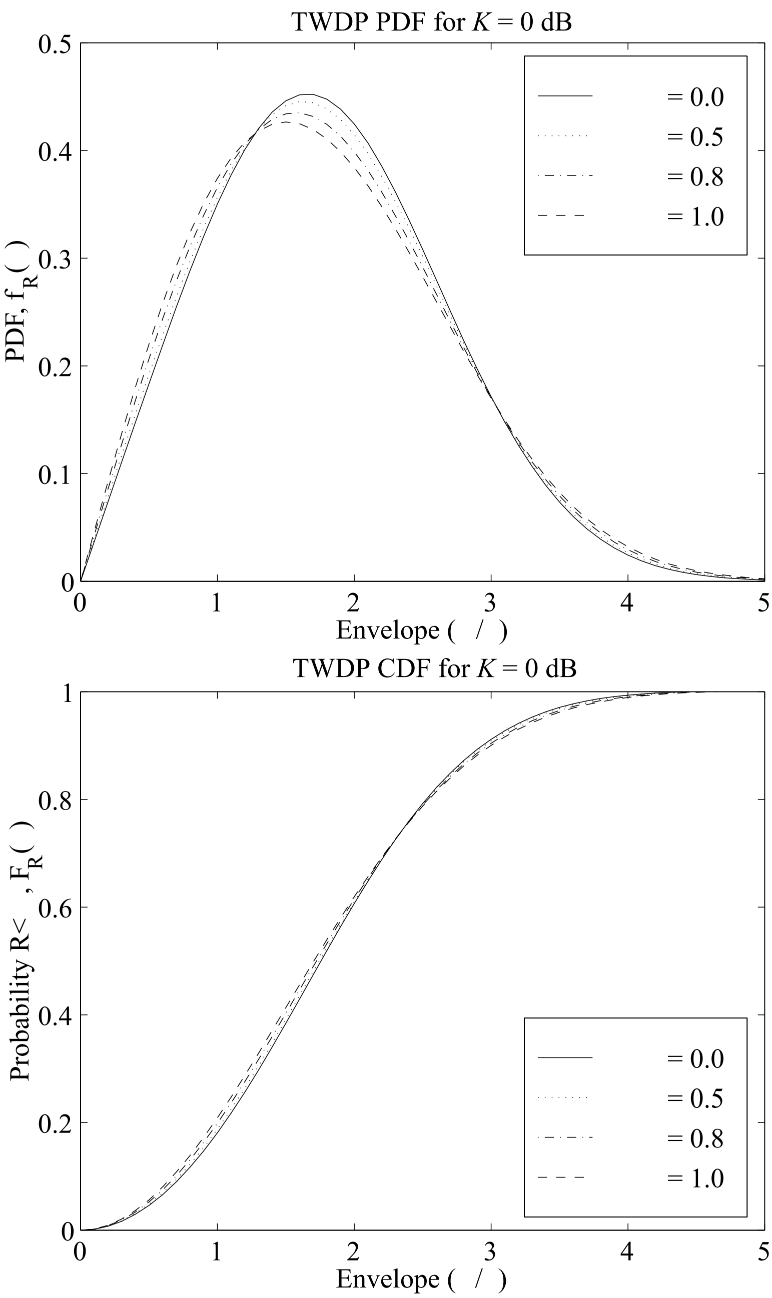

Figure 5.8 TWDP PDF and CDF for $K = 0$ dB [Dur02] ($\sigma = \sqrt{P_{\mathrm{dif}}/2}$).

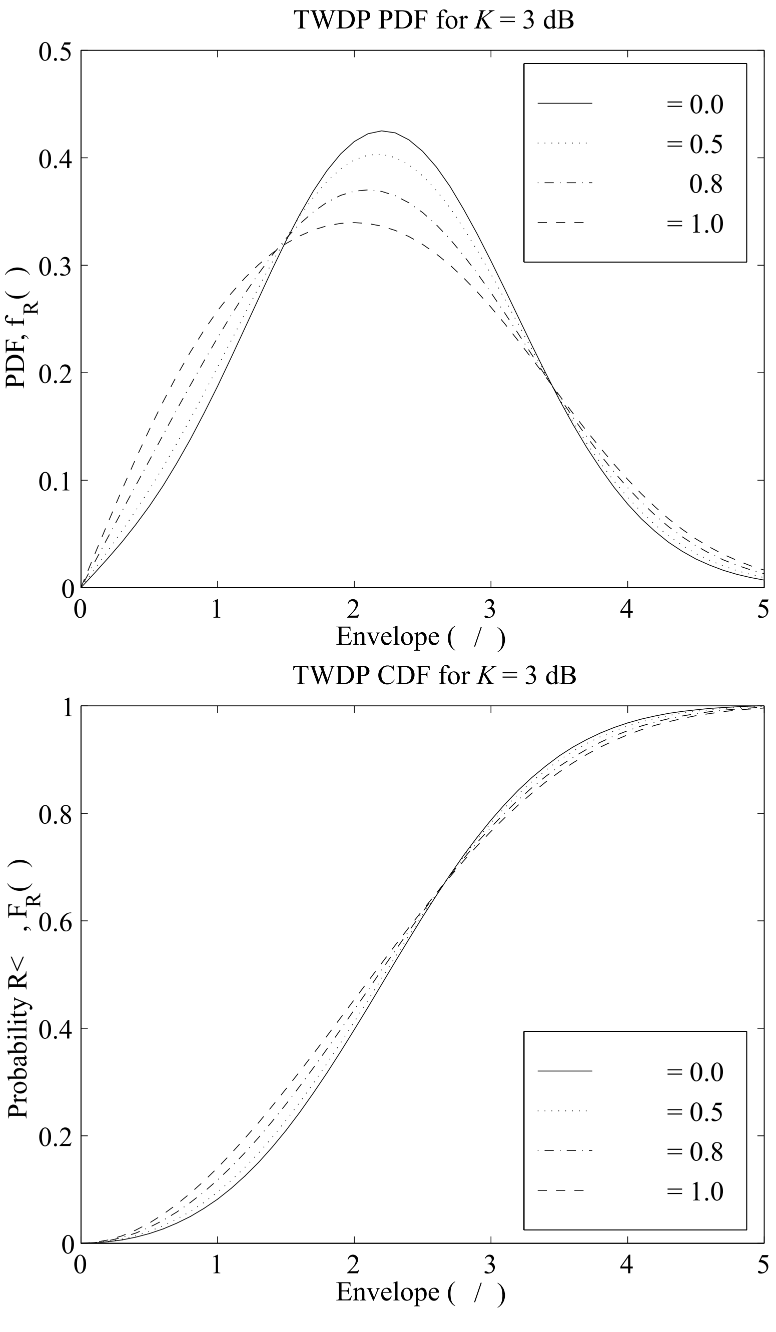

Figure 5.9 TWDP PDF and CDF for $K = 3$ dB [Dur02] ($\sigma = \sqrt{P_{\mathrm{dif}}/2}$).

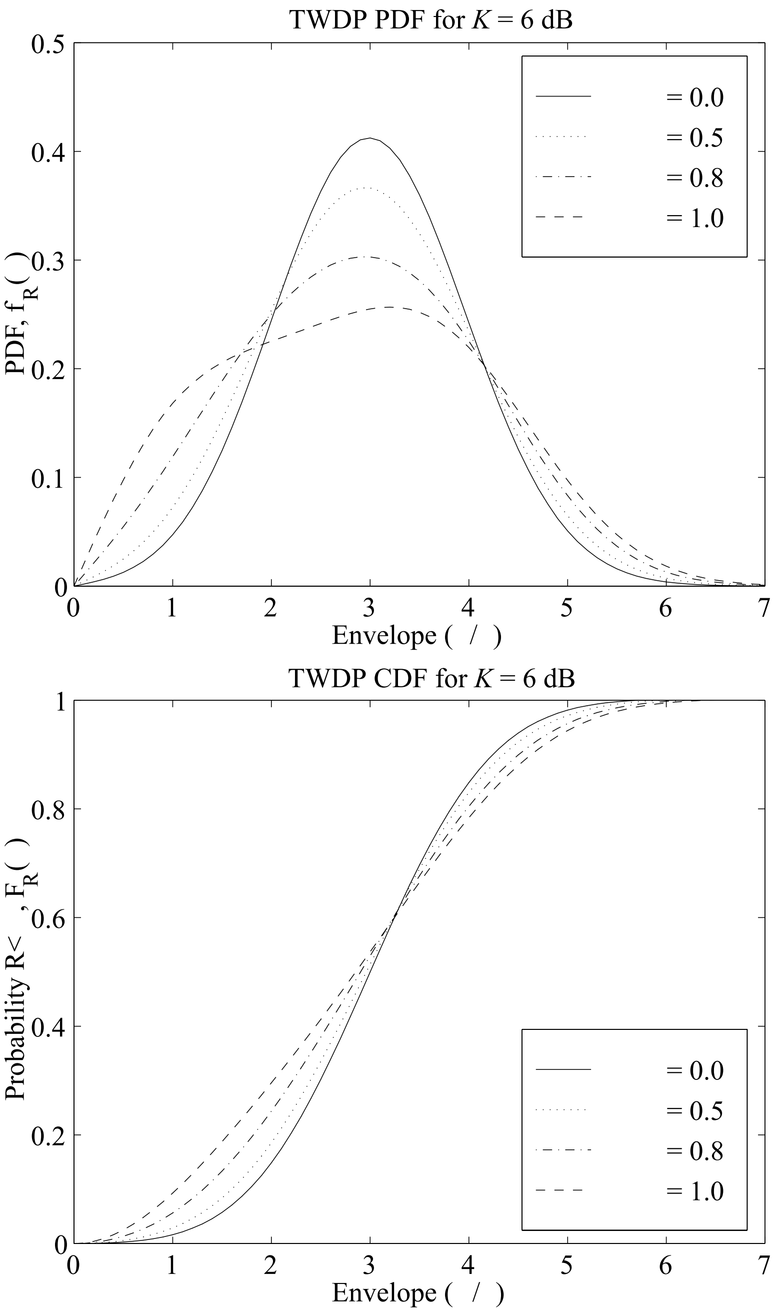

Figure 5.10 TWDP PDF and CDF for $K = 6$ dB [Dur02] ($\sigma = \sqrt{P_{\mathrm{dif}}/2}$).

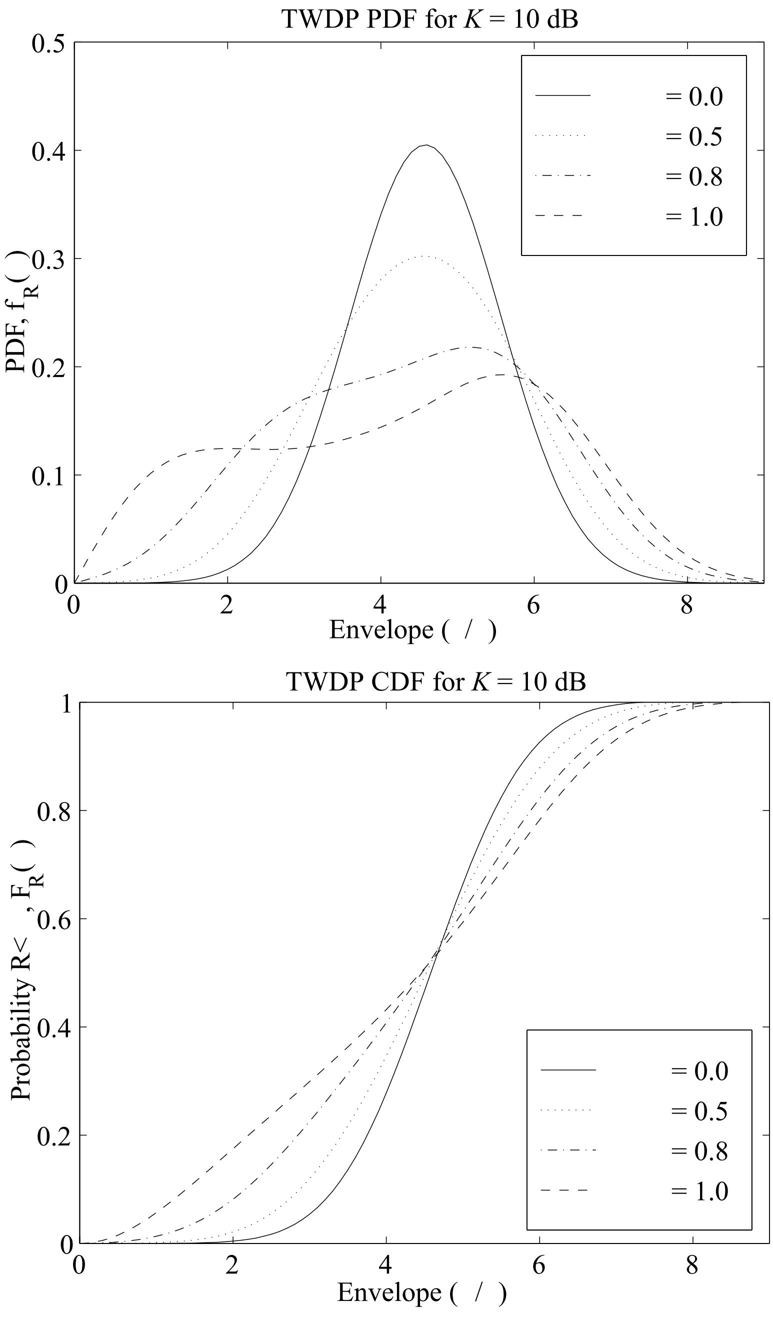

Figure 5.11 TWDP PDF and CDF for $K = 10$ dB [Dur02] ($\sigma = \sqrt{P_{\rm dif}/2}$).

This condition derives from Figure 5.6, which shows that Rician PDFs resemble the shapes of Rayleigh PDFs (after scaling) for a Rician K-factor less than 0 dB. Under this condition, the entire sum of voltage components may be treated together as diffuse, nonspecular power, despite the presence of two specular components.

The Rician and Rayleigh approximation conditions, therefore, are best summarized in terms of the TWDP K and Δ parameters by the following:

$$\text{Rician Condition:} \quad K < \frac{2}{\Delta} \tag{5.4.5}$$

$$\text{Rayleigh Condition:} \quad K < \min\left(\frac{2}{\Delta}, \frac{1}{\sqrt{1-\Delta^2}} - 1\right) \tag{5.4.6}$$

These conditions show the parameter range over which a TWDP PDF may be approximated by an analytically simpler Rician or Rayleigh PDF. If these conditions are not met, then the only recourse is to use Equation (5.4.2) or some other evaluation of Equation (5.2.13) for $N = 2$ and nonzero P_{dif}.

Table 5.4 shows three examples of TWDP fading and determines the simplest approximate PDF that describes the voltage envelope of each. Case A in Table 5.4 satisfies the Rayleigh condition of Equation (5.4.6). Case B, on the other hand, satisfies only the Rician condition of Equation (5.4.5). Case C satisfies neither condition and may not be approximated by a Rayleigh or Rician PDF. Note how the subtle changes in voltage amplitudes between the three cases drastically affects the overall shape and calculation of the PDF, emphasizing the need for careful and accurate representation of TWDP PDFs. See Example 5.4 for another example of finding the optimum PDF representation.

Table 5.4 Three Examples of TWDP Fading That May Simplify to Rayleigh or Rician PDFs

	Example TWDP Voltage Values					
	1^{st} Specular	2^{nd} Specular	Diffuse RMS	Parameters		Simplest
Case	Voltage (V_1)	Voltage (V_2)	Voltage ($\sqrt{P_{\text{dif}}}$)	K	Δ	PDF
A	2 μV	2 μV	3 μV	0.89	1.0	Rayleigh
B	4 μV	2 μV	3 μV	2.22	0.8	Rician
C	4 μV	4 μV	3 μV	3.56	1.0	TWDP

Example 5.4: PDF Grouping

Problem: It is known that an I-SLAC model is composed of three multipath waves with voltage amplitudes 4 μV, 3 μV, and 2 μV and a diffuse, nonspecular component with $P_{\text{dif}} = (1\mu\text{V})^2$. Find the simplest analytical representation, if any, of this envelope PDF.

Solution: Perform the following steps to ascertain the best PDF:

1. The initial grouping of voltages is $[V_1 = 4,\ V_2 = 3,\ V_3 = 2,\ P_{\text{dif}} = 1]$ (units dropped for simplicity).
2. There is diffuse power ($P_{\text{dif}} \neq 0$) and there are more than two specular components ($N = 3$), so all but the two largest specular components must be grouped with the nonspecular component. The new grouping is $[V_1 = 4,\ V_2 = 3,\ P_{\text{dif}} = 5]$.
3. The TWDP factors for this distribution are $K = 5$ and $\Delta = 0.96$. This TWDP distribution is too complicated to simplify to a Rayleigh distribution ($K > 1$) or a Rician distribution ($K\Delta > 1$), but can be approximated accurately by Equation (5.4.2) ($K\Delta < 10$).
4. The value of $\left\lceil \frac{K\Delta}{2} \right\rceil$ is 3, so an order-3 approximation of Equation (5.4.2) should be used to represent the PDF.

5.4.4 TWDP PDF Applications

The TWDP PDF and its approximations are important for characterizing fading in a variety of propagation scenarios. Small-scale fading is characterized by the TWDP PDF whenever the received signal contains two strong, specular multipath waves. While this may occur for typical narrowband receiver operation, directional antennas and wideband signals increase the likelihood of TWDP small-scale fading.

The use of directive antennas or arrays at a receiver, for example, amplifies several of the strongest multipath waves that arrive in one particular direction while attenuating the remaining waves [God97], [Win98]. This effectively increases the ratio of specular to nonspecular received power, turning a Rayleigh or Rician fading channel into a TWDP fading channel.

Wideband signal fading will likely exhibit TWDP fading characteristics for similar reasons. A wideband receiver has the ability to reject multipath components that arrive with largely different propagation time delays [Rap02a], [Bra91]. This property of a wideband receiver separates specular multipath components from other nonspecular multipath waves. Under these circumstances, the ratio of specular to nonspecular received power increases for a given propagation delay and a TWDP fading channel may result.

5.4.5 Closing Remarks on TWDP Fading

Beyond the TWDP PDF, a three-wave with diffuse power (3WDP) PDF is the next logical step. The value of such an analytically difficult PDF, however, is questionable. Much like the previously discussed four-wave PDF, the central-limit theorem would begin to dominate the behavior of an I-SLAC model, making it difficult to distinguish between the different cases of a 3WDP PDF. For example, a 3WDP PDF may be approximated by the TWDP PDF if the smallest of the three specular voltage components is grouped with the nonspecular power. This approximation would fail only if the nonspecular power were small compared to the third smallest specular component - yet such a situation implies that the nonspecular power is so small that it could be ignored: A 3WDP PDF could then be approximated by the three-wave PDF. Therefore, it is safe to say that the analytical expressions of Equation (5.4.2) and Table 5.1 provide a near-complete description of the possible envelope fading of complex voltages in an I-SLAC model.

5.5 Chapter Summary

In a randomly varying small-scale channel, the distribution of received signal power or envelope dramatically affects the performance of a receiver. These fluctuations are best described using a PDF, which characterizes all of the first-order statistics of a channel. The following key points summarize the first-order analysis described in this chapter:

- Mean received power is one of the most fundamental first-order statistics in channel modeling and measurement.
  - ▷ For a U-SLAC model, the mean power of the channel is equal to the sum of the powers carried by individual multipath waves.
  - ▷ An I-SLAC model is strict-sense stationary.
  - ▷ A U-SLAC model is ergodic if its scattering is heterogeneous.
  - ▷ For a U-SLAC model with heterogeneous scattering, spatial averaging and frequency averaging produce identical results for mean received power.
- The canonical PDF generator of Equation (5.2.13) describes the distribution of received envelope voltages for I-SLAC models.
  - ▷ The generator is based on the reduced wave grouping and uses a characteristic function approach.
  - ▷ There are five closed-form solutions to the PDF generator.
  - ▷ The simplest solutions have become popular in wireless engineering.
- The two-wave with diffuse power (TWDP) PDF models the most general type of fading behavior.
  - ▷ This PDF has no closed-form solution.
  - ▷ There are several techniques for approximating the TWDP PDF.
  - ▷ The TWDP PDF contains Rayleigh, Rician, one-wave, and two-wave PDFs as special cases.
  - ▷ TWDP behavior can deviate substantially from Rayleigh or Rician PDFs.

Envelope PDF calculation completely characterizes the first-order power statistics of a random radio channel. While useful, first-order statistics do not provide any information as to how processes develop as a function of frequency and space. To understand the space-varying characteristics of random channels, we will further develop our analysis of the 3D spatial channel and introduce the concept of multipath *angle spectrum*. This is the subject of Chapter 6.

PROBLEMS

1. The following statistic, χ, is used to describe a frequency-varying I-SLAC model, $\tilde{h}(f)$:

$$\chi(f_1, f_2, f_3) = \mathrm{E}\left\{\tilde{h}(f_1)\tilde{h}^*(f_2)\tilde{h}(f_3)\right\}$$

Demonstrate how it is possible to simplify the number of dependencies in this statistic.

2. You decide to measure local area power using two techniques. First, you measure the spatial average of a narrowband channel, $\tilde{h}(\vec{\mathrm{r}})$. Then, you measure the frequency average of a fixed channel, $\tilde{h}(f)$. Explain a possible physical interpretation for the multipath waves if the two averages do not agree.

3. Why are the following functions invalid for use as an envelope PDF?

a. $f_R(\rho) = \frac{1}{\sigma\sqrt{2\pi}} \exp\left(-\frac{\rho^2}{2\sigma^2}\right)$

b. $f_R(\rho) = \mathrm{u}(\rho - 1) - \mathrm{u}(\rho - 3)$

c. $f_R(\rho) = \mathrm{sn}(\rho - 3)\mathrm{u}(\rho)$

d. $f_R(\rho) = \mathrm{sn}^2(\rho)\mathrm{u}(\rho)$

4. Transform the following envelope PDFs into power PDFs based on the relationship $p = \rho^2$:

a. Weibull PDF: $f_R(\rho) = a\exp(-ap)\,\mathrm{u}(p), \quad a > 0$

b. Half-Gaussian PDF: $f_R(\rho) = \frac{1}{\sigma}\sqrt{\frac{2}{\pi}} \exp\left(-\frac{\rho^2}{2\sigma^2}\right)\mathrm{u}(\rho)$

c. Two-Wave PDF: $f_R(\rho) = \frac{2\rho}{\pi\sqrt{4V_1^2V_2^2 - (V_1^2 + V_2^2 - \rho^2)^2}}$, for $|V_1 - V_2| \leq \rho \leq V_1 + V_2$

d. Rician PDF: $f_R(\rho) = \frac{2\rho}{P_{\mathrm{dif}}} \exp\left(\frac{-\rho^2 - V_1^2}{P_{\mathrm{dif}}}\right) \mathrm{I}_0\left(\frac{2V_1\rho}{P_{\mathrm{dif}}}\right)\mathrm{u}(\rho)$

e. Half Sinc-Squared PDF: $f_R(\rho) = 2V_0\mathrm{sn}^2(V_0\rho)\mathrm{u}(\rho)$

5. Transform the following power PDFs into envelope PDFs based on the relationship $p = \rho^2$:

a. Exponential: $f_P(p) = \frac{1}{P_0}\exp\left(-\frac{p}{P_0}\right)\mathrm{u}(p)$

b. Half-Gaussian PDF: $f_P(p) = \frac{1}{\sigma}\sqrt{\frac{2}{\pi}} \exp\left(-\frac{p^2}{2\sigma^2}\right)\mathrm{u}(p)$

c. Triangle PDF: $f_P(p) = 2(1 - p)[\mathrm{u}(p) - \mathrm{u}(p - 1)]$

d. Half Sinc-Squared PDF: $f_P(p) = 2P_0\mathrm{sn}^2(P_0 p)\mathrm{u}(p)$

6. Recall the transmission line problem from previous engineering courses. A lossless transmission line of length $L = l\lambda$ and real impedance, Z_0, terminates in a complex load with impedance, $\tilde{Z}_L$. This configuration is illustrated below:

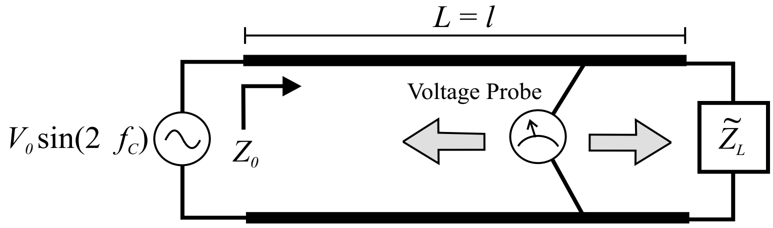

The transmission line is very long, and a voltage probe takes measurements at random positions along the length of the line. Find an expression for the envelope PDF measured by the probe in terms of l, Z_0, and $\tilde{Z}_L$.

7. Write a computer program to numerically compute any PDF from the I-SLAC PDF generator of Equation (5.2.13). Use this program to graph the PDFs for the following cases:

a. $N = 4$, $V_1 = V_2 = V_3 = V_4 = 1\text{V}$, $P_{\text{dif}} = 1\text{V}^2$

b. $N = 4$, $V_1 = V_2 = V_3 = V_4 = 1\text{V}$, $P_{\text{dif}} = 0$

c. $N = 4$, $V_1 = V_2 = 2V_3 = 2V_4 = 1\text{V}$, $P_{\text{dif}} = 0$

d. $N = 3$, $V_1 = V_2 = 2V_3 = 1\text{V}$, $P_{\text{dif}} = 1\text{V}^2$

e. $N = 3$, $V_1 = 2V_2 = 2V_3 = 1\text{V}$, $P_{\text{dif}} = 1\text{V}^2$

8. Consider a local area propagation scenario where three equal-amplitude specular waves ($V_1 = V_2 = V_3 = 1\text{V}$) are received in the presence of other diffuse multipath waves with total power P_0. We may can calculate this case by either grouping one of the specular voltages with the diffuse power (a TWDP approximation) or using the full 3WDP representation:

$$\begin{array}{llll} \text{TWDP:} & V_1 = V_2 = 1\text{V} & \text{3WDP:} & V_1 = V_2 = V_3 = 1\text{V} \\ & P_{\text{dif}} = P_0 + 1\text{V}^2 & & P_{\text{dif}} = P_0 \end{array}$$

Evaluate and graph both the exact 3WDP and approximate TWDP envelope PDFs for different values of P_0. At which value of P_0 does this approximation fail?

9. Use the Rayleigh PDF to calculate the following information about a Rayleigh fading channel with average power P_{dif}:

a. What is the mean of the Rayleigh fading envelope?

b. What is the most likely value of the envelope?

c. What is the *median* of the envelope? (The median is the voltage, ρ_m, at which $\Pr[R > \rho_m] = \Pr[R < \rho_m] = 0.5$.)

10. Analytically write and solve the generating integral for the Rician PDF. Hint: See Appendix A.4 for formulas that help evaluate this integral.

11. Prove that the following mathematical relationship holds for any positive values of A_i:

$$\int_0^\infty \int_0^\infty x^3 \nu \prod_{i=1}^{N} \mathrm{J}_0(A_i \nu) \mathrm{J}_0(\nu x) \, d\nu \, dx = \sum_{i=1}^{N} A_i^2$$

Hint: Try applying some theorems learned in this chapter before computing any integrals.

12. Prove that the Rician distribution may be approximated as a Gaussian distribution for $K \gg 1$. (See Table A.3 in Appendix A.)

13. Which of the following descriptions of wave groupings will produce envelopes that never fade to zero?

a. $\{V_i\} = \{4, 3, 2, 1\}$

b. $\{V_i\} = \{4, 2, 1\}$

c. $\{V_i\} = \{1, 3, 4, 10, 1\}$

d. $\{V_i\} = \{200, 1, 1\}$ and $P_{\mathrm{dif}} = 0.1\mathrm{V}^2$

14. Compute $\mathrm{E}\{P\}$ for the groups of waves in the previous problem.

15. Assume that N specular waves with equal amplitude are received by an antenna. Test how the exact I-SLAC PDF compares with an approximation of the PDF using the Rayleigh distribution of equal power. Graph the cases for $N = 3, 4, 5, 7, 10, 15$, and 20.

5.A Envelope Characteristic Functions

In the study of PDFs, it is convenient to define a characteristic function, which is the Fourier transform of the PDF [Pap91]. The standard mathematical definitions for finding a characteristic function, $\Phi_X(\upsilon)$, from a PDF, $f_X(x)$, and vice versa are given below:

$$\Phi_X(\upsilon) = \int_{-\infty}^{+\infty} f_X(x) \exp(-j\upsilon x)\, dx \tag{5.A.1}$$

$$f_X(x) = \frac{1}{2\pi} \int_{-\infty}^{+\infty} \Phi_X(\upsilon) \exp(j\upsilon x)\, d\upsilon \tag{5.A.2}$$

Characteristic functions are useful for studying the addition of independent random variables. If random variables A, B, and C satisfy the relationship $C = A + B$ and A and B are independent, then their characteristic functions satisfy the relationship $\Phi_C(\upsilon) = \Phi_A(\upsilon)\Phi_B(\upsilon)$ [Sta94].

Characteristic functions are also useful for studying the superposition of two independent random voltages, such as those in the SLAC model. Since voltage, $\tilde{V}$, is complex-valued, its characteristic function must be a *double* Fourier transform over the joint PDF of the random in-phase, X, and quadrature, Y, voltage components ($\tilde{V} = X + jY$). This transformation is demonstrated below:

$$\Phi_{XY}(\upsilon_x, \upsilon_y) = \int_{-\infty}^{+\infty}\int_{-\infty}^{+\infty} f_{XY}(x, y) \exp(-j\upsilon_x x) \exp(-j\upsilon_y y)\, dx\, dy \tag{5.A.3}$$

$$f_{XY}(x, y) = \frac{1}{4\pi^2} \int_{-\infty}^{+\infty}\int_{-\infty}^{+\infty} \Phi_{XY}(\upsilon_x, \upsilon_y) \exp(j\upsilon_x x) \exp(j\upsilon_y y)\, d\upsilon_x\, d\upsilon_y \tag{5.A.4}$$

Starting with the basic envelope PDF, $f_R(\rho)$, as a function of only envelope, ρ, it is possible to extend this PDF into a joint PDF using the relationship

$$f_{R\Phi}(\rho, \phi) = \frac{1}{2\pi\rho} f_R(\rho) \tag{5.A.5}$$

Equation (5.A.5) is a joint PDF, albeit in terms of envelope, ρ, and phase, ϕ, variables instead of in-phase, x, and quadrature, y, variables. Equation (5.A.5) assumes that the net phase, ϕ, is uniformly distributed, independent of ρ - consistent with the I-SLAC model.

Rather than convert Equation (5.A.5) into an XY joint PDF, it is more convenient to make a change of variables in the transform definition of Equation (5.A.3). With the polar-coordinate substitutions $x = -\rho\cos\phi$, $y = -\rho\sin\phi$, and $dx\, dy =$

$\rho\, d\rho\, d\phi$, Equation (5.A.3) becomes

$$\Phi_{XY}(\upsilon_x, \upsilon_y) = \frac{1}{2\pi} \int_0^{\infty} \int_0^{2\pi} f_R(\rho) \exp(j\upsilon_x \rho \cos\phi) \exp(j\upsilon_y \rho \sin\phi)\, d\phi\, d\rho \tag{5.A.6}$$

Equation (5.A.6) may be grouped:

$$\Phi_{XY}(\upsilon) = \int_0^{\infty} f_R(\rho) \left[\frac{1}{2\pi} \int_0^{2\pi} \exp\left[-j\upsilon\rho\cos(\phi + \phi_0)\right] d\phi \right] d\rho \tag{5.A.7}$$

where $\upsilon = \sqrt{\upsilon_x^2 + \upsilon_y^2}$ and $\tan(\phi_0) = \upsilon_y/\upsilon_x$. The angle ϕ_0 is unimportant, since the integration of ϕ_0 is over the entire period of the cosine function in Equation (5.A.7). Thus, the characteristic function is solely dependent on the variable υ.

The bracketed term in Equation (5.A.7) is a standard definite integral that evaluates to a zero-order Bessel function of the first kind [Gra94]. The final expression for the transformation from envelope PDF to characteristic function is Equation (5.2.3). Using a similar set of reductions, the reverse transformation from characteristic function to envelope PDF becomes Equation (5.2.4). The only assumption made in these transformations is the statistical independence and uniform distribution of the complex voltage phase.